Available online at www.sciencedirect.com

ScienceDirect

Procedia Structural Integrity 47 (2023) 765–781

Structural Integrity Procedia

www.elsevier.com/locate/procedia

27th International Conference on Fracture and Structural Integrity (IGF27)

FEM analysis of NiTi rotary endodontic instruments to fatigue stress conditions: influence of geometrical parameters and design optimization

Franco Maria Di Russo[1]*, Alessio Zanza[2], Annamaria Gisario[1], Stefano Natali[3], Giuseppe Ruta[4], Luca Testarelli[2]

[1]*Department of Mechanical and Aerospace Engineering, Sapienza University of Rome, Via Eudossiana 18, Rome 00184, Italy*
[2]*Department of Oral and Maxillo-Facial Sciences, Sapienza University of Rome, Via Caserta 6, Rome 00184, Italy*
[3]*Department of Chemical Engineering, Materials and Environment, Sapienza University of Rome, Via Eudossiana 18, Rome 00184, Italy*
[4]*Department of Structural and Geotechnical Engineering, Sapienza University of Rome, Via Eudossiana 18, Rome 00184, Italy*

Abstract

The aim of this paper was to analyse the mechanical behaviour of NiTi endodontic rotary instruments when subjected to fatigue stresses. Four different commercial endodontic files, characterized by different cross-section shapes, were tested. Two finite element models were built to identify the cross-section shape with the best performance. In the first FEM model, rotary instruments were fixed near the tip, while a transverse displacement was applied to the bottom. Von Mises equivalent stresses were evaluated to compare the bending response of the different instruments. In the second FEM model the low-cycle fatigue life of these instruments was examined, when constrained to displace in a curved root canal and contemporary rotate. The comparison of the results, in terms of cyclic fatigue, allowed to identify the commercial instrument whose particular geometric conformation ensures better mechanical strength under test conditions. Subsequently, an analysis of geometry parameters influences on the fatigue life was performed and a design optimization was carried out. In the design optimization process, the output parameter is the total deformation. The results obtained showed that it is possible to achieve an increase in fatigue life of up to 50%. Finally, the fatigue life of the optimized geometry has furthermore tested in a double curvature root canal.

Keywords: Nickel-Titanium, Fatigue, Endodontics, optimization

* Corresponding author.
E-mail address: francomaria.dirusso@uniroma1.it

10.1016/j.prostr.2023.07.042

1. Introduction

The diffusion of NiTi rotary endodontic instruments represented the most significant technological innovation in endodontics. Its introduction, in fact, has profoundly changed root canal instrumentation, so much so that it can be considered the technological revolution that sanctioned the birth of Modern Endodontics (Walia et al., 1988). The mechanical characteristics offered by the NiTi alloy, in fact, have contributed to the spread of new rotary files that have replaced traditional steel hand tools. The traditional tools were used by applying a manual axial movement. Being very thin and not very tapered instruments, there were difficulties in reaching the apex of the root. This inevitably led to irregularities when working the canal, resulting in the risk of failure of the final seal. The use of rotary instruments with increased taper allowed to obtain perfectly tapered canals, drastically increasing the probability of a successful treatment outcome (Brotzu et al., 2014). Nowadays, almost all endodontic files are produced with Nickel-Titanium alloy, a shape memory alloy known as SMA. The introduction of the NiTi alloy as the material of choice for the production of rotary endodontic instruments has enabled a considerable increase in the level of predictability and success rates, around 95%, for root canal therapies (Chércoles-Ruiz et al., 2017; Walia et al., 1988). Among the characteristics that make this alloy particularly suitable for the manufacture of rotating endodontic instruments are its biocompatibility and resistance to corrosion (Fife et al., 2004); shape memory, the ability to recover its original shape, when deformed, by means of heat input; superelasticity, being able to withstand large reversible deformations in the elastic field. The latter two properties are attributable to the austenite-martensite dysplastic transformation, which can be induced either by a change in temperature or by a state of stress acting on the material (Brotzu et al., 2014; Duerig et al., 1999; S. et al., 2010). NiTi alloy, in fact, has two different crystallographic phases, called austenitic phase and martensitic phase (El-Anwar et al., 2015, p.; T. O. Kim et al., 2009). This innovation has contributed to the introduction of more technologically advanced tools, which are remarkably high-performance in terms of cutting capacity and can withstand higher physical stresses. Resistance to bending and torsional stresses remains the greatest limitation in the use of NiTi rotary instruments. Continuous rotation within pronounced curves results in stresses that are far greater than those resulting from manual use, which, despite the favourable properties of the NiTi alloy, can lead to intraoperative fracture more frequently than with manual use of steel files (Madarati et al., 2013). Despite Nickel-Titanium alloy shows unique mechanical properties, the instruments used in rotary endodontic preparation are subjected to particularly high stresses. That correspond to high structural stresses that could lead to intraoperative fracture of the instrument and thus, from a clinical point of view, result in iatrogenic error (Ismail et al., 2019; H. C. Kim et al., 2009). In order to avoid intra-canal separation, manufacturers have focused on improving the mechanical capabilities of these instruments, with the aim of overcoming the fracture, the greater limitation. Innovations have always been driven towards improving the flexibility and strength of the instruments through the use of different sectional designs, the introduction of innovative heat treatments or manufacturing processes, or through the development of better performing cutting blades. Cyclic fatigue fracture is due to the contributions of tensile and compressive forces to which the instrument is subjected during rotation in a curved canal. Once the elastic capacity of the alloy is exceeded, the tool is irreversibly deformed until fracture occurs (Peters, 2004; Plotino et al., 2009). In the second case, fracture occurs when a portion of the instrument, most often the tip, stuck between the dentinal walls of the root canal, while the most coronal portion continues to rotate. Once the material's elasto-plastic deformation capabilities have been exceeded, the instrument will undergo a crash fracture (Sattapan et al., 2000a, 2000b). Torsional fracture, in fact, is generally characterized by macroscopic distortion or unwinding of the splines adjacent to the area where the fracture occurs (Brotzu et al., 2014). The accumulation of cyclic fatigue causes micro-cracks to form on the surface of the file (Kim et al., 2013). Geometrical discontinuities, porosity, inclusions, and overheating verified during the production phase represent additional weakening factors (Galal and Hamdy, 2020). Fatigue fracture is difficult to predict, as macroscopic signs do not arise before fracture. The fatigue life of endodontic instruments, regardless of their structure and the stress levels to which they are subjected, is quite limited and does not exceed 500 cycles (Fife et al., 2004; Inan et al., 2007; Robertson et al., 2012). All manufacturers suggest a limited time of use for each instrument to avoid intraoperative fracture. Thus, current endodontic instruments are afflicted by phenomena that affect their structural integrity. The abrupt appearance of fracture, especially in the case where it is due to fatigue accumulation, makes it impossible to determine an appropriate length of operating range. In recent years, much attention has been paid to heat treatments and instrument mass, and the experiments conducted have almost always been conducted under static conditions. While useful in defining the basic mechanical properties of NiTi instruments,

the clinical relevance of these tests has been considered very low ("Mechanical Tests, Metallurgical Characterization, and Shaping Ability of Nickel-Titanium Rotary Instruments: A Multimethod Research," 2020; Zanza et al., 2021a). Only recently have studies been conducted concerning the influence of some geometrical aspects, such as the relevance of mass distribution with respect to the axis of rotation or the shear efficiency of geometrically different cross sections. In this case, however, the constraint conditions were aimed at describing the case of torsion resistance (Seracchiani et al., 2022; Zanza et al., 2021b).

One way to achieve a more reliable mechanical performance evaluation is to conduct dynamic analyses, which take into account the influence of geometric factors throughout the treatment: from insertion of the device into the canal and shaping. From a numerical point of view, phenomena of this kind can be analysed using finite element simulation tools. It is possible to reproduce the mechanical and structural behaviour of such devices in a scenario more in accordance with the clinical case, focusing on the influence relationships that exist between geometric factors and overall performance.

The purpose of this study, then, is to evaluate the mechanical behaviour of some of the most popular commercial endodontic instruments under two different conditions: replicating static test conditions inherent to flexibility and, then, imposing sliding and rotational conditions within a simplified reproduction of the real root canal. Next, an analysis of the influence of geometric attributes on fatigue accumulation is to be conducted, and a Design Optimization procedure with the aim of increasing resistance to the fatigue phenomenon is carried out.

2. Material and method

2.1. Material

Material properties used for this analysis refer to a material model well known in the literature, the "Auricchio Model," which is widely used within this type of study for both SMA and superelastic materials (Auricchio, 2001; Prados-Privado et al., 2018). Assuming the adoption of a NiTi alloy with an austenitic crystal structure, relevant material properties are shown in Table 1.

Table 1. – NiTi alloy material properties (Auricchio, 2001)

Parameter	Magnitude
Young's modulus of austenite	42.53 GPa
Austenite Poisson's ratio	0,33
Young's Modulus of Martensite	12.828 GPa
Martensite Poisson's ratio	0.33
Uni-axial transformation strain	6%
Slope of the stress-temperature curve for loading	6.7
Start of transformation loading	492 MPa
End of transformation loading	630 MPa
Reference temperature	22 °C
Slope of the stress-temperature curve for unloading	6.7
Start of transformation unloading	192 MPa
End of transformation unloading	97 MPa
End of martensitic elastic regime	1200 MPa

This material model was then implemented in Ansys, in the "Engineering Data" section. Superelasticity properties were introduced through the "Superelasticity" tool.

2.2. Geometries

Selected rotary endodontic instruments for this paper were reproduced using commercial CAD modeling software "Dassault Systems Solidworks 2021." The modeling procedure used reverse engineering logic by measuring the characteristics of each instrument and subsequent reproduction in the CAD environment. Table 2 shows the salient geometric features.

Table 2. – Geometrical characteristics of selected rotary files

File	Edge length [mm]	Tip diameter [mm]	Taper	Cross-section shape	Pitch
Reciproc	16	0,25	8%	Italic S-shaped	4,5 threads (1600°)
Wave One	16	0,25	7%	Triangular	4 thread (1260°)
Wave One Gold	16	0,25	$D_0 – D_4$: 7% $D_4 – D_{12}$: 6% $D_{12} – D_{16}$: 3%	Parallelogrammic	4,2 threads (1400°)

The helix pitch is expressed in terms of numbers of threads but it is also reported in terms of degrees, corresponding to the twist function imposed to the active part of the file to reproduce the helicoid into the 3D model.

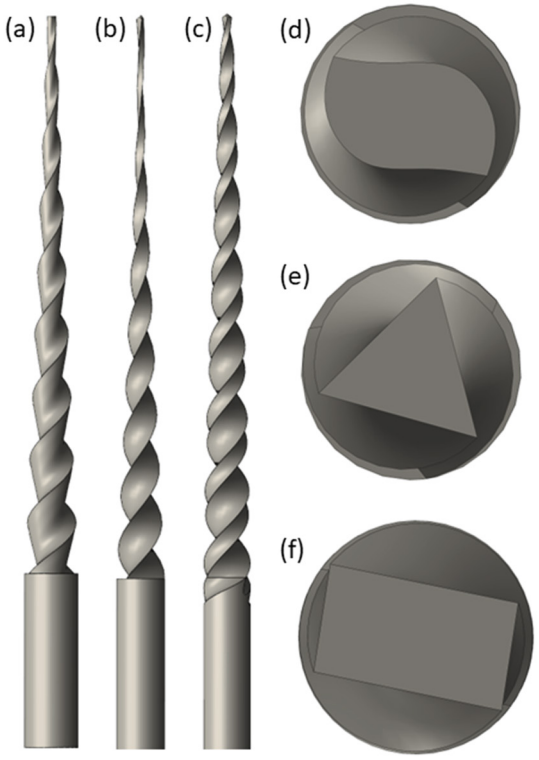

Figure 1. 3D model and cross-section shape of selected rotary files: (a) Reciproc; (b) Wave One; (c) Wave One Gold; (d) Reciproc cross-section; (e) Wave One cross-section shape; (f) Wave One Gold cross-section shape.

2.3. Analysis of fatigue behavior using the Coffin-Manson model

Dealing with fatigue failure, in most cases, it is introduced the Wohler curve. This curve, found on an S-N (stress-number-of-cycles) graph, relates the maximum amplitude of cyclically applied stress to the number of cycles the material can withstand. This type of approach, however, is more suitable for cases where the number of cycles is very large; it goes as far as talking about millions of cycles (HCF). For rotating NiTi endodontic instruments, it is appropriate to deal with oligo-cyclic fatigue (LCF), considering that the number of cycles completed before reaching failure is very limited. The standard used to describe this phenomenon will be the Coffin - Manson criterion. It is based on estimating the number of cycles to failure, having as input the total strain of the material (Oltmans, n.d.; Runciman et al., 2011). The total strain is given by the sum of the elastic and plastic strain. The two terms in the second member of the following equation are the elastic and plastic strain, respectively:

$$\frac{\Delta\varepsilon}{2} = \frac{\Delta\varepsilon_{el}}{2} + \frac{\Delta\varepsilon_{pl}}{2}$$

Explicating the two terms to the second member gives:

$$\frac{\Delta\varepsilon}{2} = \varepsilon'_F \, \mathrm{N}^c + \frac{\sigma'_F}{E} N^b$$

Where:

N = numbers of cycles to failure

ε'_F = fatigue ductility coefficient

σ'_F = fatigue strength coefficient

σ'_F= modulo di elasticità

c = fatigue ductility exponent

b = fatigue strength exponent

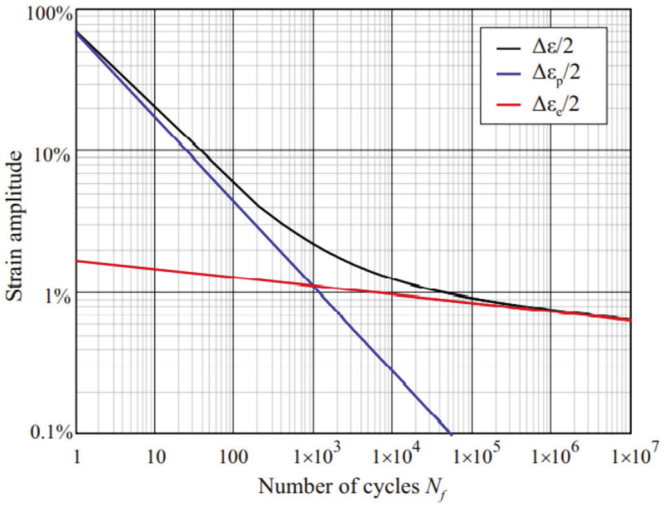

Figure 2. Graph of the Coffin - Manson equation. For a low number of cycles, the plastic part is predominant. For a high number of cycles the elastic component has more influence.(Roda-Casanova et al., 2021)

3. FE Models

The following study consists of three detached phases, to which two different finite element models correspond.

3.1. Flexibility analysis

First, a model was generated to define the flexibility capabilities of each instrument under consideration. Indeed, it is well known that the flexibility and fatigue behavior of an endodontic instrument are directly correlated parameters. Fatigue accumulation is an inevitable phenomenon for all materials subjected to alternating cyclic, tensile and compressive stresses (Plotino et al., 2009). Boundary conditions of the following analysis were defined by referring to previous studies (Galal and Hamdy, 2020; Montalvão et al., 2014; Prados-Privado et al., 2019). An interlocking constraint is imposed along the axis of the tool, for a distance of 3mm from the tip. An orthogonal displacement of 9mm is then imposed on the tang.

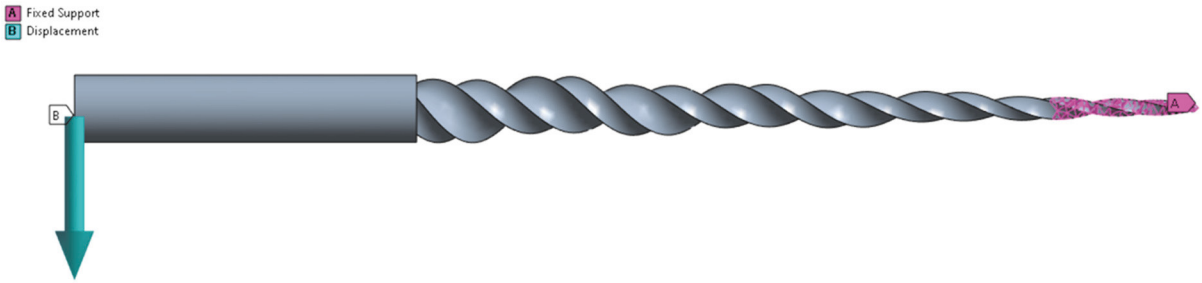

Figure 3. Boundary conditions for flexibility analysis

Discretization of the three-dimensional models was conducted by generating a rather coarse mesh at the tang. An average Element Size of 0.5 mm was selected. Instead, it is thickened on the cutting edge by imposing an element size of 0.2mm. The element type chosen is "SOLID187," 10-node tetrahedra with nonlinear behaviour. For WaveOne, 16611 nodes and 8528 elements are counted. The Wave One Gold is discretized into 18194 nodes and 9275 elements. Lastly, the Reciproc counts 36613 nodes and 20305 elements. Unlike the other commercial rotary instruments, a Sizing of 0.1 mm was adopted for the Reciproc because of the more complex geometry.

3.2. Fatigue analysis

The next analysis involves the same instruments to different operating conditions. These are forced to enter and rotate in a curved canal, a simplified representation of the actual root canal. The actual conformation of root canals is very subjective, depending specifically on the clinical case under consideration. It is not unusual to be faced with root canals with very irregular conformations and characterized by having challenging curvatures, even in different planes. For the definition of boundary conditions, reference was made to previous similar studies (El-Anwar et al., 2015; Roda-Casanova et al., 2021). Only one type of canal was adopted, with radius of curvature equal to 5 mm and inclination equal to 60° (see Figure 9).

An analysis involving two time steps was set up. During the first time step, the insertion of the endodontic instrument inside the canal is imposed through the prescription of a displacement equal to 15.5 mm. During the second time step a rotation of 360° is forced. The mesh parameters set differ from the previous case. A maximum element size of 0.5mm was set. The surfaces of the cutting edge, in contact with the canal relatives, instead have a denser mesh, with Sizing of 0.2 mm. The mesh thickening was deemed necessary because of the higher accuracy of the results. A major issue, in setting the conditions of the analysis, is the management of the contact between the surfaces of the endodontic instrument and the inner canal walls. To define the contact between the bodies as realistically as possible, a "Frictional" contact type with a friction coefficient of 0.1 was introduced. A "Nodal - Normal To Target" type of detection method was then adopted so as to solve interference problems in areas such as contact angles (Zhu, 2016). In order to make easier for the software to converge to the solution, the "Normal Stiffness" option was also

activated and set to "Factor," defining a value of 0.1. As low a "Normal Stiffness" as possible is recommended if there are convergence problems; instead, it is recommended to raise this value if too much penetration is noticed between the bodies. Finally, the "Interface treatment" option was set to "Adjust To Touch." During the simulation it may happen that, due to a mesh that is not too accurate at some critical points, contact between surfaces is not detected. Or, on the contrary, a distortion of the mesh elements may induce localized contact in a different area than one would expect.

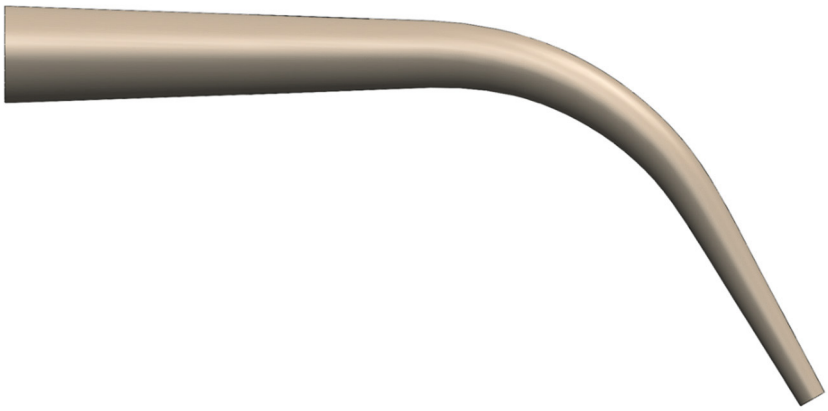

Figure 4. Single curvature shape root canal representation

Figure 5. Contact detection

3.3. Design Optimization

The Design Optimization process was conducted by making use of the fatigue behavior analysis of the instrument when it rotates within the canal. The goal is to improve the fatigue life of the rotating instruments under consideration. The parameters were chosen according to their influence on the structural behavior of the instrument and also according to the areas of maximum stress concentration. The following geometric parameters were selected: (1) the tip section diameter; (2) the section diameter 4 mm from the tip; (3) the section diameter 12 mm from the tip; and (4) the helix pitch. The Design Optimization procedure, was conducted on the Wave One Gold. The reason was due to the results obtained from commercial rotary instruments in previous analyses. The output parameter selected is "Equivalent Total Strain," evaluated at the instant of time at which the maximum value is recorded.

4. Results and discussion

4.1. Flexibility analysis

The results obtained were analyzed by comparing the Equivalent Von Mises Stress. Figure 11 shows the qualitative distribution of equivalent stresses for the three types of instruments selected, while Figure 6 shows the trends of the Equivalent Von Mises Stress. Table 3, on the other hand, displays the results in terms of the maximum equivalent stress recorded for each instrument.

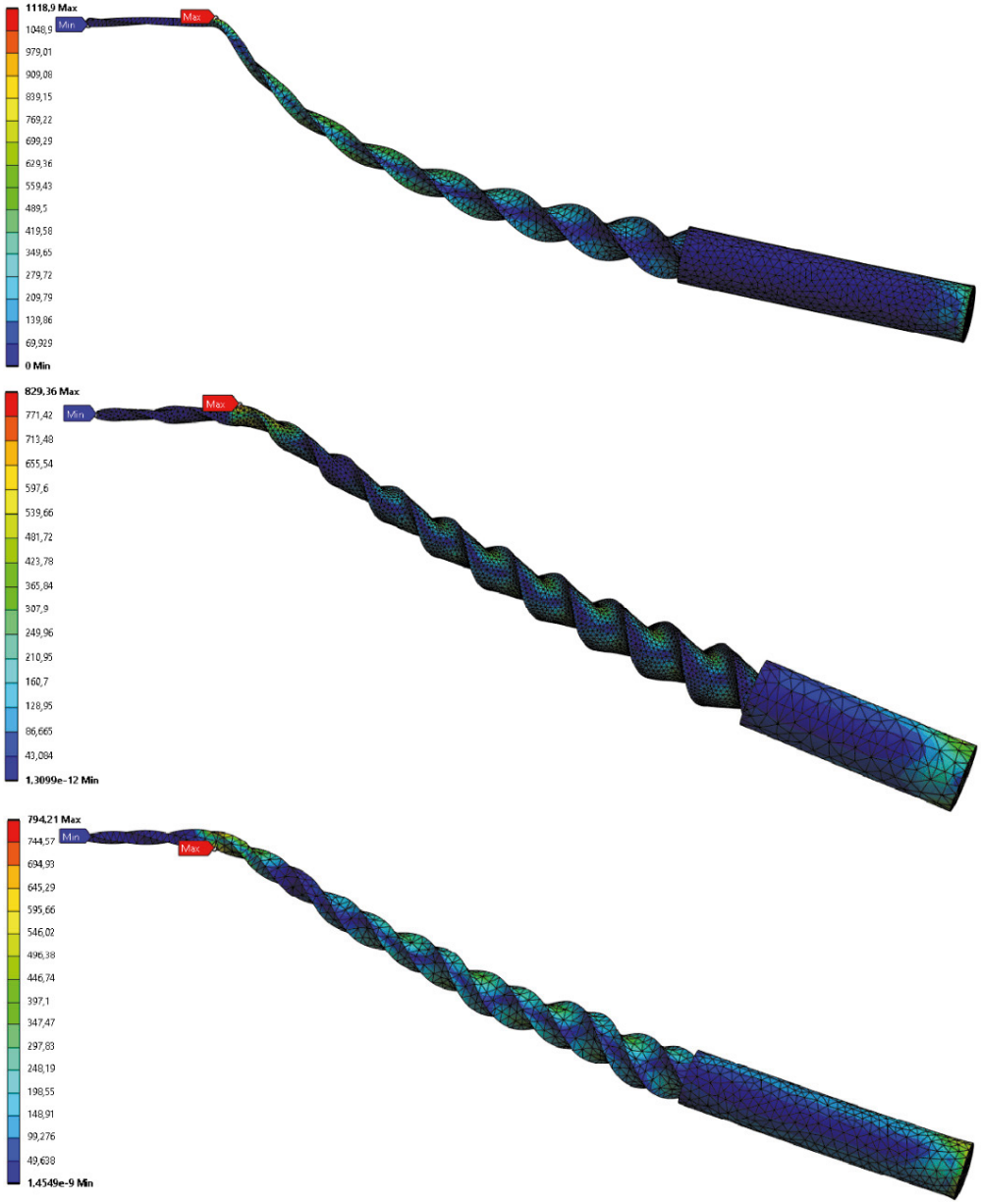

Figure 6. Equivalent Von Mises Stress distribution [MPa]: (a) Wave One; (b) Reciproc; (c) Wave One Gold

Wave One turns out to be the device most stressed by the imposed boundary conditions. Its particular geometry turns out to be the least prone to bending among the three under consideration. Reciproc and Wave One Gold, on the other hand, showed more favorable results. The maximum value achieved, shown in Table 2, is similar. The graph in Figure 7 shows that the stresses developed by Reciproc at the beginning of the test are markedly higher than those recorded by the other two devices. This gap, then, gets thinner. The Wave One will register much higher stress indices. The Wave One Gold, on the contrary, will demonstrate the development of stresses whose value will always be below that shown by the Reciproc.

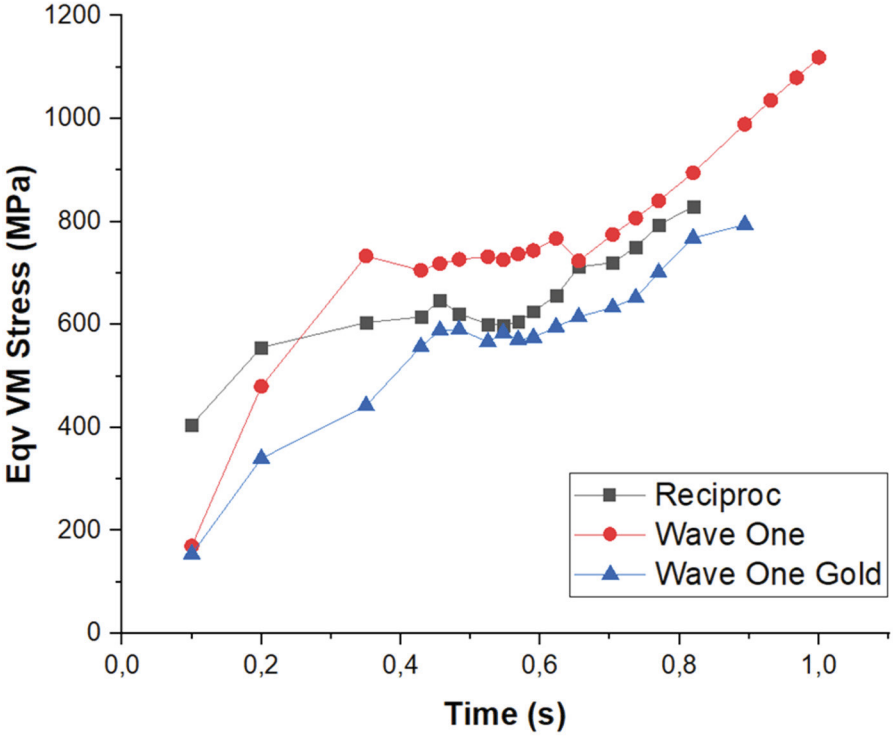

Figure 7. Equivalent Von Mises Stress trends

Table 3. – Maximum equivalent Von Mises Stress value recorded

File	Eqv Von Mises Stress [MPa]
Wave One	1118
Reciproc	829
Wave One Gold	794

4.2. Fatigue analysis

Von Mises equivalent stress distributions and total strain were considered as outputs of the analysis. The resulting stress state allows evaluation of the behavior of each individual instrument subjected to the previously introduced boundary conditions. A comparative analysis on the resulting strains allows an assessment of which of the four tools is least stressed. The maximum total strain value, on the other hand, allows a comparison on the resulting stress state in the four rotating instruments, but is also necessary for the calculation of the fatigue life of each device. The

calculated stress state and strain gradient are also a function of time, as they are evaluated throughout the test. This allows a very accurate analysis of device response to be conducted. Thus, we speak of a maximum value, for the total strain, because, for the calculation of fatigue life, the peak value reached by each device during the span of the simulation is identified and selected. In all four cases, the time interval within which the maximum strain value is recorded is that in which the instrument, inserted in the canal, rotates. Figure 8 presents the trend of equivalent stresses during the duration of the analysis. Table 4 shows the maximum equivalent stress values recorded for each instrument.

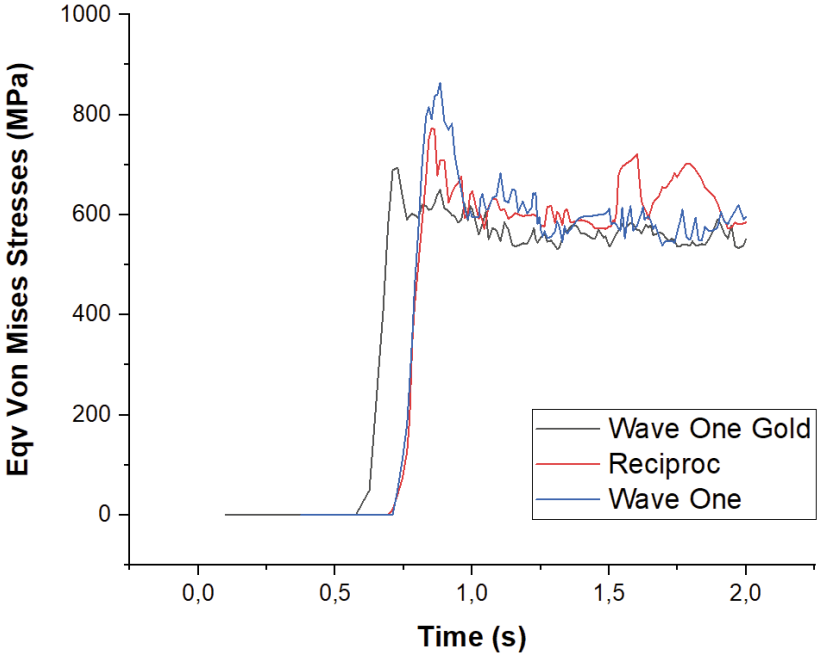

Figure 8. Equivalent Von Mises Stress trends

Table 4. – Maximum equivalent Von Mises Stress value recorded

File	Eqv. Von Mises Stress [MPa]
Wave One	863,8
Reciproc	805,45
Wave One Gold	694,41

The rotating instrument that develops the greatest stresses is the Wave One, which registers a maximum value of 863 MPa. The one that experiences lower stresses is the Wave One Gold with 694 MPa.

Figure 9 shows the equivalent stress distributions at the instant when the peak value is reached. The point of maximum stress is variable among the four endodontic instruments, but always located at a distance of 2 mm to 3 mm from the tip.

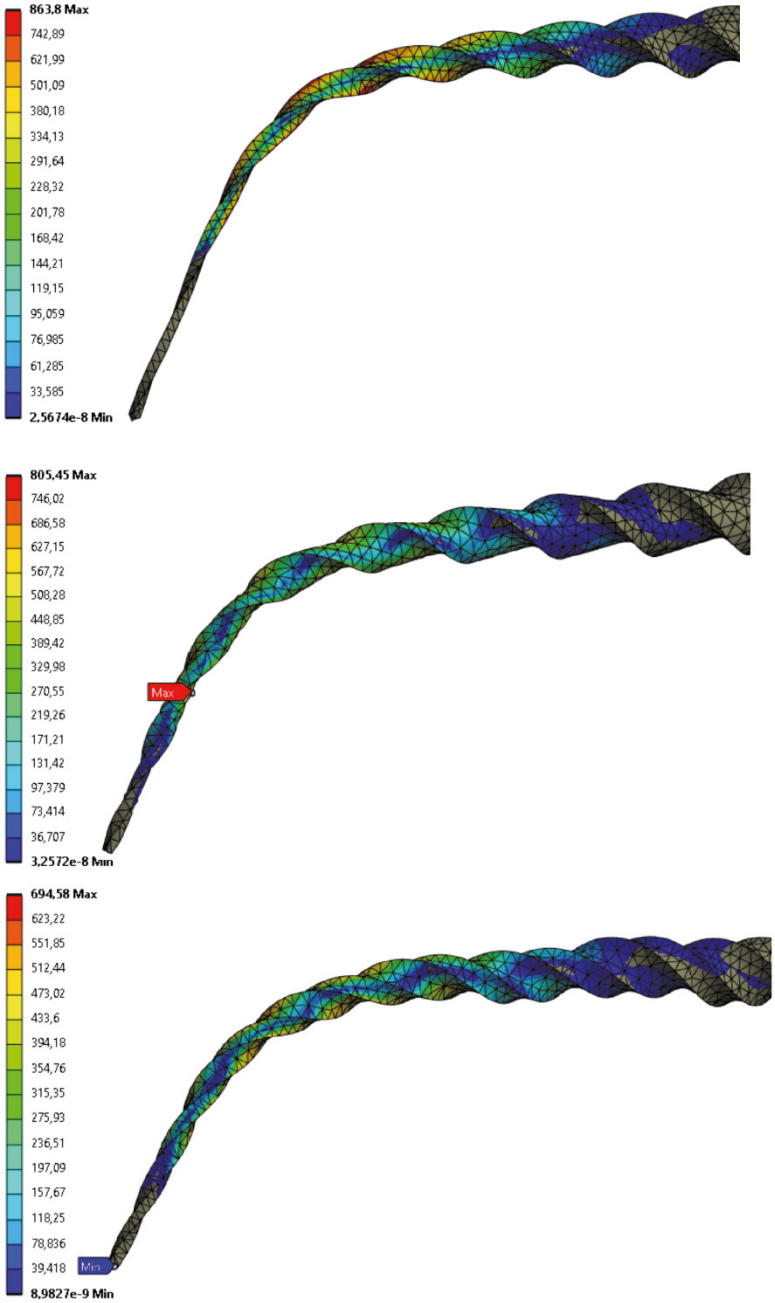

Figure 9. Equivslent Von Mises Stress distribution: (a) Wave One; (b) Reciproc; (c) Wave One Gold

Similarly, the maximum total strains exhibited by each instrument are presented in Table 4, and Figure 10 shows the evolution of the Total Strain value during the time interval of the analysis.

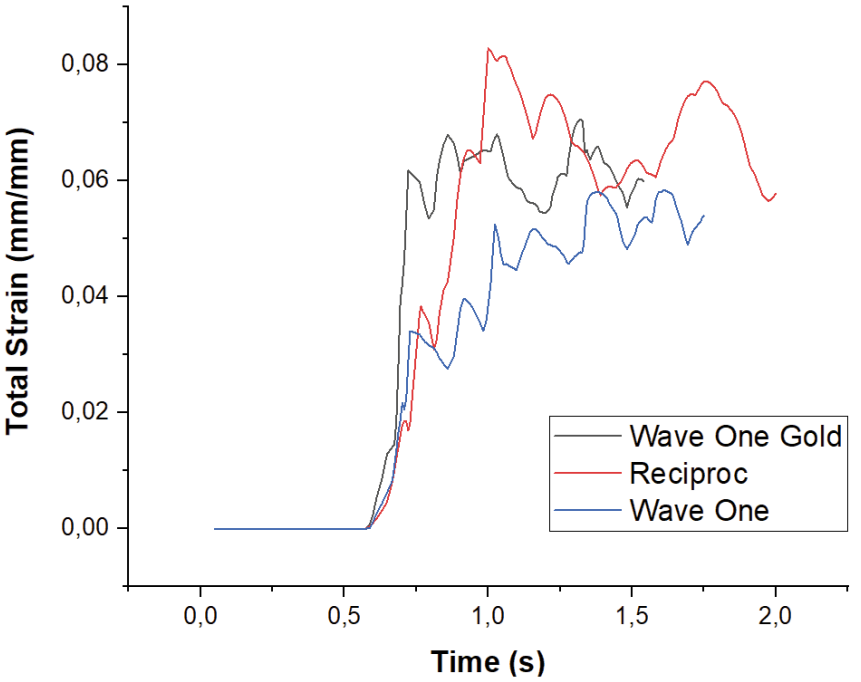

Figure 10. Equivalent Total Strain trends [mm/mm]

Table 5. – Maximum equivalent Total Strain value recorded

File	Eqv. Von Mises Stress [MPa]
Wave One	0,0584
Reciproc	0,0829
Wave One Gold	0,0706

Reciproc records the highest strain, with 0.0829 mm/mm. In contrast, Wave One records the lowest value. Figure 11 shows the areas of the four instruments subjected to deformation, at the instant of time when, for each instrument, the maximum value was recorded.

Along the axis of the instrument, in the affected areas, the stress distributions shown are due to a superposition of phenomena. Acting, in fact, will be bending stresses, due to bending induced by the conformation of the canal, and tension-compression stresses, due to rotation. The friction generated in the contact between the cutting edges on the shank of the devices and the inner walls of the canal will trigger a phenomenon such that there will be a constant alternation of compressive and tensile stresses along the axis of the instrument.

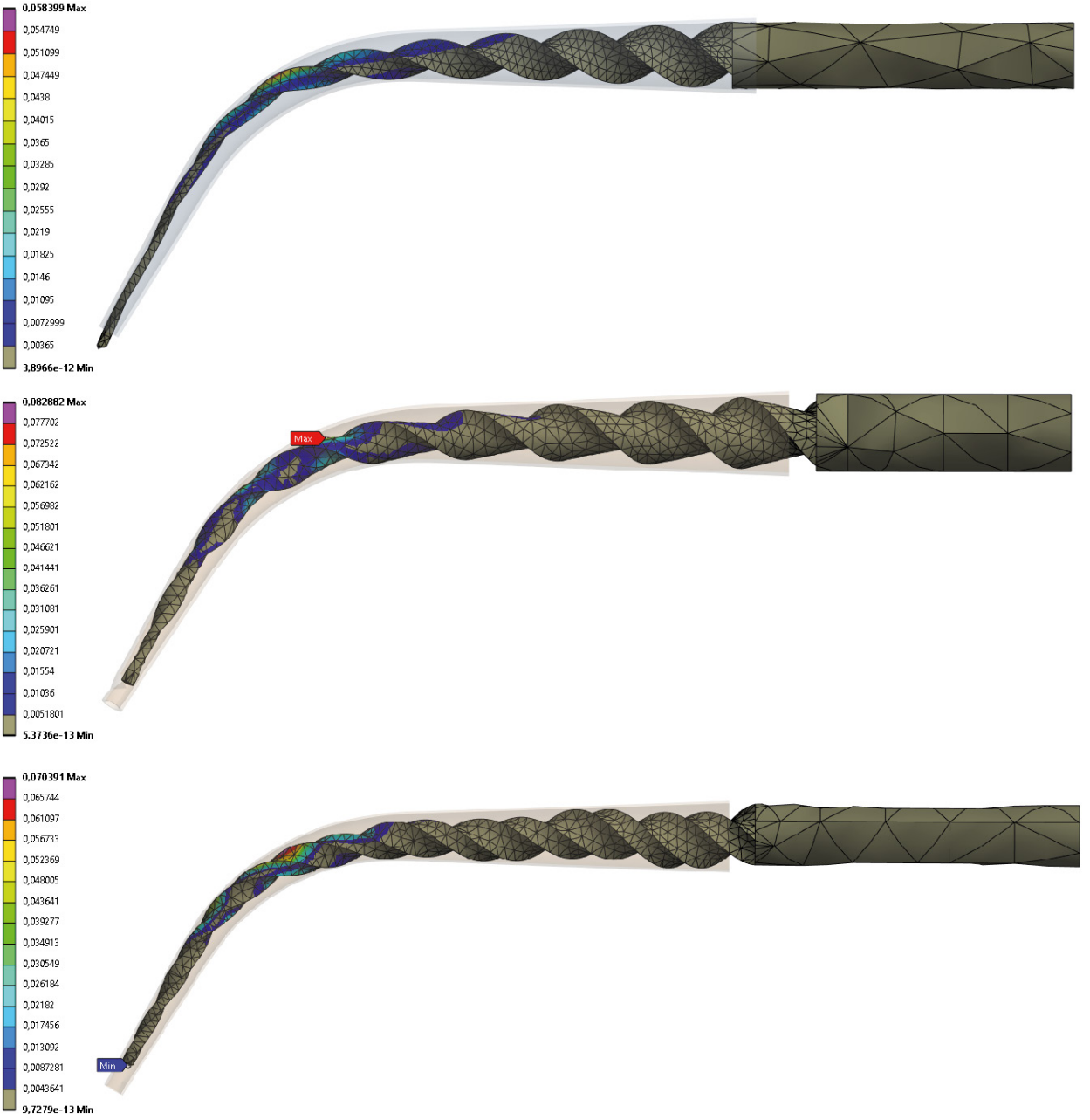

Figure 11. Equivalent Total Strain distribution: (a) Wave One; (b) Reciproc; (c) Wave One Gold

4.3. Design Optimization

For each selected input geometric parameter, a range of variability was defined having the original value as reference. For diameter at tip, cross-section diameter at 4mm and at 12mm, a range of 10 values with 1mm pitch was established. Five values below the original value of 0.25mm and five values above. A range of 10 values was also

always considered for the pitch of the cutting edges. To optimize the timing required by the optimization procedure, considering the multitude of combinations (10^4 plausible combinations), a study was conducted on the influence of the variation of each individual parameter on the overall mechanical behavior. The results were always evaluated as a function of the total strain values recorded by each iteration. In this way, 40 analyses were conducted, from which an optimal value was extracted for each parameter.

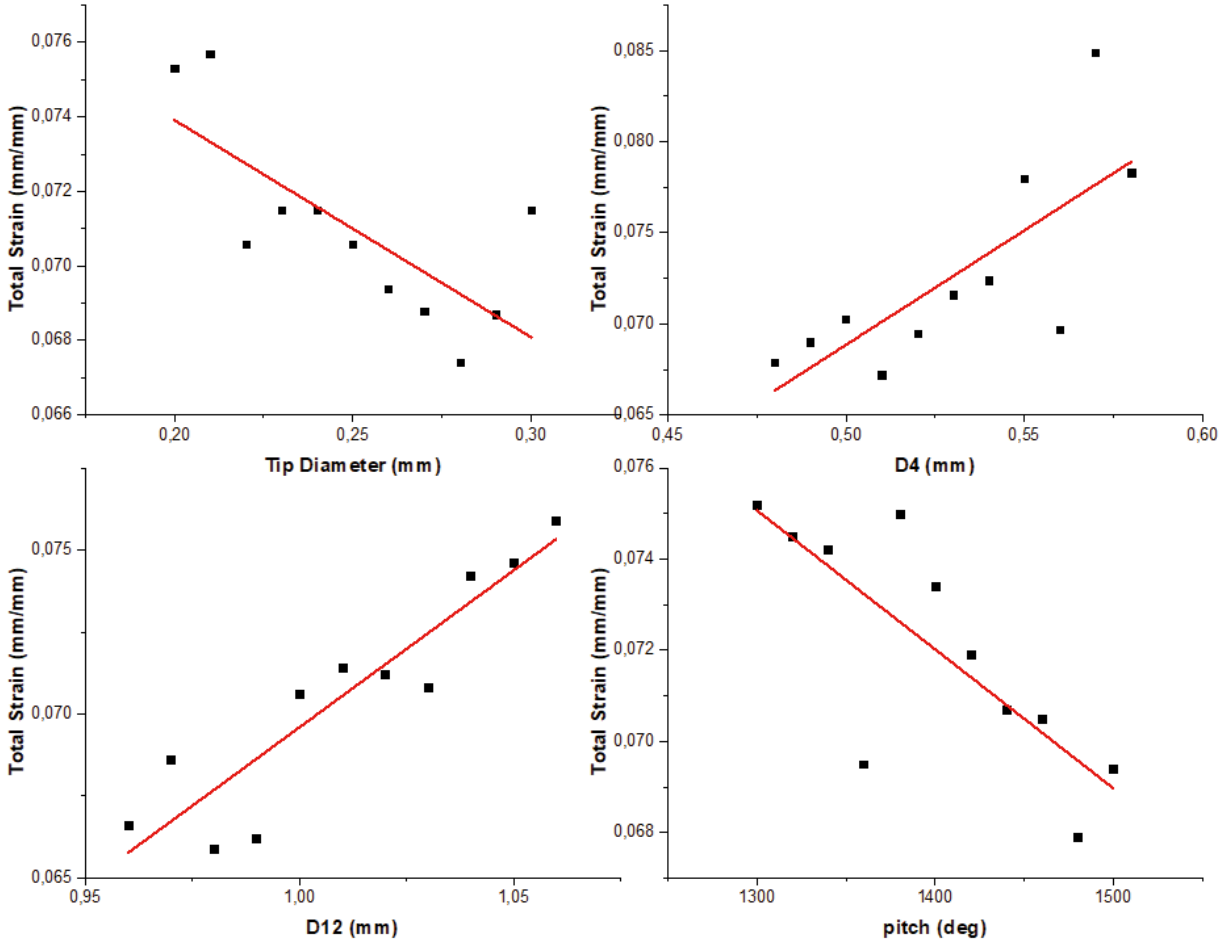

Figure 12. Trend of total strain as a function of selected parameters: (a) Tip Diameter; (b) Cross-section diamater at 4mm; (c) Cross-section diameter at 12 mm; (d) Helix pitch

The graphs shown in Figure 12 clearly describe how, as the value taken by the selected parameters changes, the value of Total Strain varies. In detail, there is an inverse proportionality relationship in the case of tip diameter. As this value increases, Total Strain decreases. Different case for the cross-sectional diameters evaluated at 4 mm and 12 mm from the tip. In this case the influence ratio is directly proportional. Finally, with regard to pitch, the resulting trend manifests a decrease in Total Strain as pitch decreases. The higher the value expressed in degree, the lower will be the pitch value expressed in mm. Please note that the value of the pitch is expressed in degrees as the input value used for generating the helical profile in the 3D model.

Sets of 3 values, centered on the optimal value, were then selected for each parameter. These new sets constituted the values assumed by the four variables in a combinatorial optimization cycle. In total, therefore, the simulation went on to calculate 81 possible combinations. Again through comparison from the Equivalent Total Strain value, the optimal combination was selected, i.e., that combination of parameter values that minimizes the total strain value. The values assumed by the parameters in the optimal configuration are shown below in Table 6 and compared with the

original values of the commercially available instrument. It can be seen from the following comparison that a less pronounced taper of the instrument favors the mechanical strength of the device. Regarding the pitch of the helical helix constituting the cutting edges of the device, it appears desirable to increase the pitch slightly for improved fatigue behavior. This, in fact, induces a reduction in the surface area of the cutting edges in contact with the canal walls.

Table 6. – Parameters value comparison between commercial configuration and optimized configurations

File	Tip diameter [mm]	4mm cross-section diameter [mm]	12mm cross-section diameter [mm]	Pitch [deg]	Eqv. Total Strain [mm/mm]
Commercial configuration	0,25	0,53	1,01	1400	0,0706
Optimized configuration	0,28	0,5	0,98	1460	0,06023

From the following result, the fatigue cycles endured by the device can be defined through the Coffin-Manson equation. The following values are entered for NiTi: : ε_F' = 0.68, σ_F' = 750 MPa, E = 42.5 GPa, c = - 0.6, b = - 0.06 (Cheung et al., 2011). The number of fatigue life cycles calculated according to the Coffin-Manson criterion for the commercial instrument and the optimized instrument are shown in Table 7.

Table 7. Fatigue life comparison between commercial configuration and optimized configurations

File	Eqv. Total Strain [mm/mm]	Fatigue Life
Commercial configuration	0,0706	288
Optimized configuration	0,06023	431

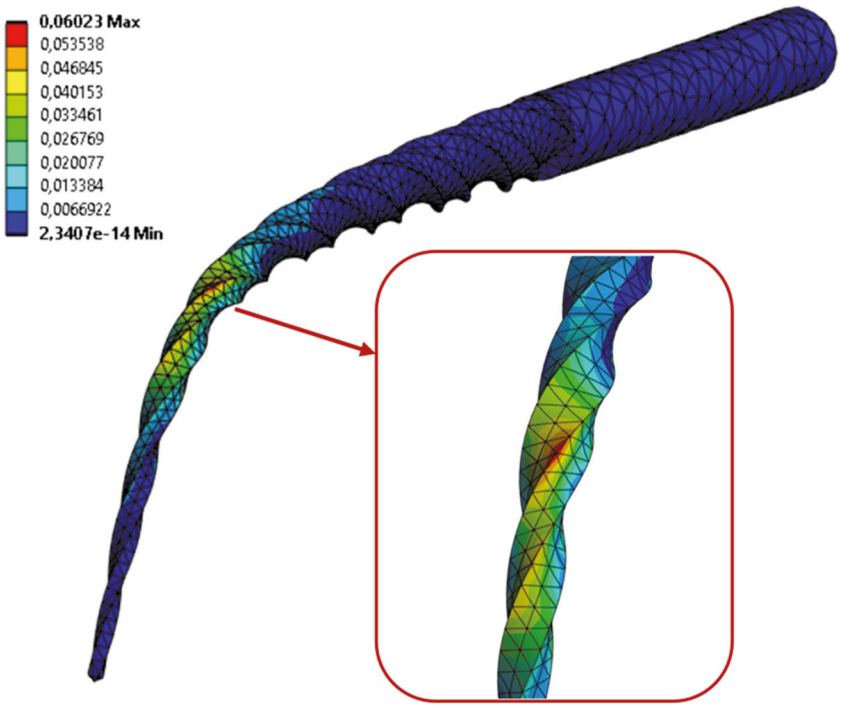

Figure 13. Equivalent Total Strain distribution on the Optimized Wave One Gold shape

Figure 13 shows the total strain gradient to which the optimized tool is subjected, with a focus on the zone subjected to the most severe conditions. The area that reaches the peak value is very localized, at the edge of the cutting edge about 3 mm away from the tip.

5. Conclusions

The present work was conducted in the spirit of preliminarily investigating the behavior of Nickel-Titanium rotary endodontic instruments through a comparative analysis concerning the behavior of instruments of different geometric design when subjected to similar working conditions as in real life. Emphasis was placed on investigating fatigue strength, which is primarily responsible, along with torsional stresses, for the occurrence of instrument fracture. An initial simulation model concerning the analysis of the flexibility properties of the different designs under analysis was generated. Through a comparison of the results obtained with those stated by previous studies, it was possible to calibrate the finite element model. Subsequently, a sharper finite element model was generated. It was imposed that the devices under consideration were induced to fit and rotate within a curved canal, a first approximation representation of the actual root canal. From the results obtained, the instrument whose design registered better mechanical strength under the imposed boundary conditions was selected. The Wave One Gold was selected. Before setting up the Design Optimization procedure, a study of the influence of the geometrical parameters, selected for the subsequent optimization procedure, on the overall mechanical behavior of the device was conducted. Ultimately, a Design Optimization procedure was conducted with the aim of exploring a possible increase in the fatigue life of the device. From the results obtained, the fatigue life of the Wave One Gold was increased by 49.6 percent, from 288 cycles of the commercial configuration to 431 cycles of the optimized configuration.

6. References

Auricchio, F., 2001. A robust integration-algorithm for a ®nite-strain shape-memory-alloy superelastic model. International Journal of Plasticity.

Brotzu, A., Felli, F., Lupi, C., Vendittozzi, C., Fantini, E., 2014. Fatigue behavior of lubricated Ni-Ti endodontic rotary instruments. Frattura ed Integrità Strutturale 8, 19–31. https://doi.org/10.3221/IGF-ESIS.28.03

Chércoles-Ruiz, A., Sánchez-Torres, A., Gay-Escoda, C., 2017. Endodontics, Endodontic Retreatment, and Apical Surgery Versus Tooth Extraction and Implant Placement: A Systematic Review. Journal of Endodontics 43, 679–686. https://doi.org/10.1016/j.joen.2017.01.004

Cheung, G.S.P., Zhang, E.W., Zheng, Y.F., 2011. A numerical method for predicting the bending fatigue life of NiTi and stainless steel root canal instruments: A numerical method for predicting the bending fatigue life of NiTi. International Endodontic Journal 44, 357–361. https://doi.org/10.1111/j.1365-2591.2010.01838.x

Duerig, T., Pelton, A., Stöckel, D., 1999. An overview of nitinol medical applications. Materials Science and Engineering: A 273–275, 149–160. https://doi.org/10.1016/S0921-5093(99)00294-4

El-Anwar, M.I., Mandorah, A.O., Yousief, S.A., Soliman, T.A., El-Wahab, T.M.A., 2015. A finite element study on the mechanical behavior of reciprocating endodontic files. Braz. J. Oral Sci. 14, 52–59. https://doi.org/10.1590/1677-3225v14n1a11

Fife, D., Gambarini, G., Britto, L.R., 2004. Cyclic fatigue testing of ProTaper NiTi rotary instruments after clinical use. Oral Surgery, Oral Medicine, Oral Pathology, Oral Radiology, and Endodontology 97, 251–256. https://doi.org/10.1016/j.tripleo.2003.08.010

Galal, M., Hamdy, T.M., 2020. Evaluation of stress distribution in nickel-titanium rotary instruments with different geometrical designs subjected to bending and torsional load: a finite element study. Bull Natl Res Cent 44, 121. https://doi.org/10.1186/s42269-020-00377-x

Inan, U., Aydin, C., Tunca, Y.M., 2007. Cyclic fatigue of ProTaper rotary nickel-titanium instruments in artificial canals with 2 different radii of curvature. Oral Surgery, Oral Medicine, Oral Pathology, Oral Radiology, and Endodontology 104, 837–840. https://doi.org/10.1016/j.tripleo.2007.06.019

Ismail, A.G., Zaazou, M.H.A., Galal, M., Kamel, N.O.M., Nassar, M.A., 2019. Finite element analysis comparing WaveOne Gold and ProTaper Next endodontic file segments subjected to bending and torsional load. Bull Natl Res Cent 43, 194. https://doi.org/10.1186/s42269-019-0215-6

Kim, H.C., Kim, H.J., Lee, C.J., Kim, B.M., Park, J.K., Versluis, A., 2009. Mechanical response of nickel-titanium instruments with different cross-sectional designs during shaping of simulated curved canals. International Endodontic Journal 42, 593–602. https://doi.org/10.1111/j.1365-2591.2009.01553.x

Kim, Hee-Chul, Hwang, Y.-J., Jung, D.-W., You, S.-Y., Kim, Hyeon-Cheol, Lee, W., 2013. Micro-Computed Tomography and Scanning Electron Microscopy Comparisons of Two Nickel-Titanium Rotary Root Canal Instruments Used With Reciprocating Motion: Shaping ability of single-file technique using reciprocating motion. Scanning 35, 112–118. https://doi.org/10.1002/sca.21039

Kim, T.O., Cheung, G.S.P., Lee, J.M., Kim, B.M., Hur, B., Kim, H.C., 2009. Stress distribution of three NiTi rotary files under bending and torsional conditions using a mathematic analysis. International Endodontic Journal 42, 14–21. https://doi.org/10.1111/j.1365-2591.2008.01481.x

Madarati, A.A., Hunter, M.J., Dummer, P.M.H., 2013. Management of Intracanal Separated Instruments. Journal of Endodontics 39, 569–581.

https://doi.org/10.1016/j.joen.2012.12.033
Mechanical Tests, Metallurgical Characterization, and Shaping Ability of Nickel-Titanium Rotary Instruments: A Multimethod Research, 2020. 46.
Montalvão, D., Shengwen, Q., Freitas, M., 2014. A study on the influence of Ni–Ti M-Wire in the flexural fatigue life of endodontic rotary files by using Finite Element Analysis. Materials Science and Engineering: C 40, 172–179. https://doi.org/10.1016/j.msec.2014.03.061
Oltmans, B., n.d. A Study of the effects of strain on NiTi shape memory alloy.
Peters, O., 2004. Current Challenges and Concepts in the Preparation of Root Canal Systems: A Review. Journal of Endodontics 30, 559–567. https://doi.org/10.1097/01.DON.0000129039.59003.9D
Plotino, G., Grande, N.M., Cordaro, M., Testarelli, L., Gambarini, G., 2009. A Review of Cyclic Fatigue Testing of Nickel-Titanium Rotary Instruments. Journal of Endodontics 35, 1469–1476. https://doi.org/10.1016/j.joen.2009.06.015
Prados-Privado, M., Gehrke, S.A., Rojo, R., Prados-Frutos, J.C., 2018. Complete mechanical characterization of an external hexagonal implant connection: in vitro study, 3D FEM, and probabilistic fatigue. Med Biol Eng Comput 56, 2233–2244. https://doi.org/10.1007/s11517-018-1846-8
Prados-Privado, M., Rojo, R., Ivorra, C., Prados-Frutos, J.C., 2019. Finite element analysis comparing WaveOne, WaveOne Gold, Reciproc and Reciproc Blue responses with bending and torsion tests. Journal of the Mechanical Behavior of Biomedical Materials 90, 165–172. https://doi.org/10.1016/j.jmbbm.2018.10.016
Robertson, S.W., Pelton, A.R., Ritchie, R.O., 2012. Mechanical fatigue and fracture of Nitinol. International Materials Reviews 57, 1–37. https://doi.org/10.1179/1743280411Y.0000000009
Roda-Casanova, V., Pérez-González, A., Zubizarreta-Macho, Á., Faus-Matoses, V., 2021. Fatigue Analysis of NiTi Rotary Endodontic Files through Finite Element Simulation: Effect of Root Canal Geometry on Fatigue Life. JCM 10, 5692. https://doi.org/10.3390/jcm10235692
Runciman, A., Xu, D., Pelton, A.R., Ritchie, R.O., 2011. An equivalent strain/Coffin–Manson approach to multiaxial fatigue and life prediction in superelastic Nitinol medical devices. Biomaterials 32, 4987–4993. https://doi.org/10.1016/j.biomaterials.2011.03.057
S., Narendranath., Desai, V., Basavarajappa, S., Arun, K.V., Yadav, S.M., 2010. Hot Rolling and Ageing Effect on the Pseudoelasticity Behaviour of Ti-Rich TiNi Shape Memory Alloy. JMMCE 09, 343–351. https://doi.org/10.4236/jmmce.2010.94025
Sattapan, B., Nervo, G., Palamara, J., Messer, H., 2000a. Defects in Rotary Nickel-Titanium Files After Clinical Use. Journal of Endodontics 26, 161–165. https://doi.org/10.1097/00004770-200003000-00008
Sattapan, B., Palamara, J., Messer, H., 2000b. Torque During Canal Instrumentation Using Rotary Nickel-Titanium Files. Journal of Endodontics 26, 156–160. https://doi.org/10.1097/00004770-200003000-00007
Seracchiani, M., Reda, R., Zanza, A., D'Angelo, M., Russo, P., Luca, T., 2022. Mechanical Performance and Metallurgical Characteristics of 5 Different Single-file Reciprocating Instruments: A Comparative In Vitro and Laboratory Study. Journal of Endodontics 48, 1073–1080. https://doi.org/10.1016/j.joen.2022.05.009
Walia, H., Brantley, W.A., Gerstein, H., 1988. An initial investigation of the bending and torsional properties of nitinol root canal files. Journal of Endodontics 14, 346–351. https://doi.org/10.1016/S0099-2399(88)80196-1
Zanza, A., D'Angelo, M., Reda, R., Gambarini, G., Testarelli, L., Di Nardo, D., 2021a. An Update on Nickel-Titanium Rotary Instruments in Endodontics: Mechanical Characteristics, Testing and Future Perspective—An Overview. Bioengineering 8, 218. https://doi.org/10.3390/bioengineering8120218
Zanza, A., Seracchiani, M., Di Nardo, D., Reda, R., Gambarini, G., Testarelli, L., 2021b. A Paradigm Shift for Torsional Stiffness of Nickel-Titanium Rotary Instruments: A Finite Element Analysis. Journal of Endodontics 47, 1149–1156. https://doi.org/10.1016/j.joen.2021.04.017
Zhu, Y., 2016. This presentation contains ANSYS, Inc. proprietary information. It is not to be distributed to others.